TÜBİTAK

Turkish Journal of Botany

http://journals.tubitak.gov.tr/botany/

Research Article

Turk J Bot
(2023) 47: 256-266
© TÜBİTAK
doi:10.55730/1300-008X.2764

Protective potential of mokko lactone from *Cheilocostus speciosus* (J. Koenig) C.D.Specht (Costaceae) rhizomes against fulminant hepatic failure

Ahmed E. ALTYAR[1,2], Ikhlas A. SINDI[3], Dina S. EL-AGAMY[4], Wael M. ELSAED[5], Ahmed M. SHEHATA[6,7], Hossam M. ABDALLAH[8,9], Gamal A. MOHAMED[8], Abdelsattar M. OMAR[10,11,12], Sabrin R. M. IBRAHIM[13,14,*]

[1]Department of Pharmacy Practice, Faculty of Pharmacy, King Abdulaziz University, Jeddah, Saudi Arabia
[2]Pharmacy Program, Batterjee Medical College, Jeddah, Saudi Arabia
[3]Department of Biology, Faculty of Science, King Abdulaziz University, Jeddah, Saudi Arabia
[4]Department of Pharmacology and Toxicology, Faculty of Pharmacy, Mansoura University, Mansoura, Egypt
[5]Department of Anatomy and Embryology, Faculty of Medicine, Mansoura University, Mansoura, Egypt
[6]Department of Pharmacology and Toxicology, College of Pharmacy, Taibah University, Al-Madinah Al-Munawwarah, Saudi Arabia
[7]Department of Pharmacology and Toxicology, Faculty of Pharmacy, Beni-Suef University, Beni-Suef, Egypt
[8]Department of Natural Products and Alternative Medicine, Faculty of Pharmacy, King Abdulaziz University, Jeddah, Saudi Arabia
[9]Department of Pharmacognosy, Faculty of Pharmacy, Cairo University, Cairo, Egypt
[10]Department of Pharmaceutical Chemistry, Faculty of Pharmacy, King Abdulaziz University, Jeddah, Saudi Arabia
[11]Department of Pharmaceutical Chemistry, Faculty of Pharmacy, Al-Azhar University, Cairo, Egypt
[12]Center for Artificial Intelligence in Precision Medicines, King Abdulaziz University, Jeddah, Saudi Arabia
[13]Department of Chemistry, Preparatory Year Program, Batterjee Medical College, Jeddah, Saudi Arabia
[14]Department of Pharmacognosy, Faculty of Pharmacy, Assiut University, Assiut, Egypt

Received: 03.01.2023 • **Accepted/Published Online:** 15.05.2023 • **Final Version:** 27.07.2023

Abstract: *Cheilocostus speciosus* (Syn*: Costus speciosus*) (Crepe or spiral ginger) is one of the species of the family Costaceae that is widely used in various traditional medicines for treating various ailments. Mokko lactone (ML) belongs to the guaianolide family of sesquiterpenes, which has been separated from *C. speciosus*. It showed noticeable antiinflammation and antioxidative capacities. The current study explored the ML hepatoprotective potential against FHF (fulminant hepatic failure) in mice. FHF was successfully established using intraperitoneal injection of D-galactosamine (D-GalN, 700 mg/kg)/lipopolysaccharide (LPS, 10 µg/kg) in male Swiss-albino mice. The mice were pretreated with ML (20 or 40 mg/kg, orally) daily for five days before D-GalN/LPS challenge. Eight hours after D-GalN/LPS injection, serum and hepatic tissue were harvested for different biochemical, histologic grading, immunohistochemical, and ELISA analyses. The results have shown that D-GalN/LPS-induced massive hepatic damage that was evident through the tremendous increase in serum biochemical parameters: transaminases, γ-GT, and ALP, as well as deteriorated histopathological architecture of the liver. D-GalN/LPS created a state of oxidative damage in the hepatocytes as there was a significant rise in MDA level concurrently with depressed antioxidants as GSH (reduced glutathione), SOD (superoxide dismutase) activity, and TAC (total antioxidant capacity). Additionally, D-GalN/LPS activated NF-κB (nuclear factor kappa-B), resulting in an increase in the production of TNF-α, IL-6, and IL-1β. Interestingly, all these changes were amended by ML pretreatment, indicating the potent hepatoprotective, antioxidant, and antiinflammatory efficacy of ML against D-GalN/LPS-induced FHF. These effects could be mediated through inhibition of NF-κB/downstream cytokine signaling. Hence, ML is suggested as new candidate for the treatment of FHF.

Key words
Mokko lactone, *Costus speciosus*, acute hepatic failure, D-galactosamine/lipopolysaccharide, inflammation, health, wellbeing

1. Introduction

FHF, renowned as acute liver failure, is a deadly clinical syndrome that is featured by massive hepatocellular death without underlying preexisting hepatic disease. The pathogenic events that underlie FHF are complex and multifactorial. Clinically, this condition is accompanied by a tremendous increase in serum transaminases, jaundice, coagulopathy, and multisystem organ failure that require

* Correspondence: sabrin.ibrahim@bmc.edu.sa

emergent liver transplantation in most patients, which is the only effective treatment till now (Gong et al., 2010; Tao et al., 2019). Thus, searching for other effective treatments to increase the survival rate of FHF has become a challenge for researchers.

A combination of D-GalN and LPS has been utilized to establish a practical experimental model of FHF in mice that mimics human acute hepatic failure in the clinic. This model is widely used to explore the potential pathogenesis and therapeutic treatments of FHF. LPS binds to TLR-4 (toll-like-receptor-4) causing the activation and translocation of NF-κB (nuclear- factor kappa-B) followed by inflammatory cytokines' production as TNF-α (tumor-necrosis factor-alpha) and ILs (interleukins) which enlarge the inflammatory response (Xia et al., 2014; Li et al., 2021). Cotreatment with D-GalN is mandatory to augment the LPS lethal effect by >1000-fold causing FHF within hours. D-GalN enhances the uridine triphosphate depletion within the hepatocytes due to the UDP-D-GalN derivative formation, resulting in stopping the synthesis of macromolecules such as glycogen, protein, and RNA in the liver (Dong et al., 2017; Tao et al., 2019). This state exacerbates the generation of reactive oxygen species (ROS) and eventually hepatocytes apoptosis (Lyu et al., 2019; Mohamadi-Zarch et al., 2021).

Traditional medicine is acknowledged as the preferable primary healthcare tool in many regions (Akbar, 2020; Süntar, 2020). It is estimated that more than 87.5% of the world's population and nearly 80% of developing countries rely directly on herbal medicine for treating various health complaints (Kumar et al., 2021; WHO, 2022). Attribution of plants to humankind is extended beyond just being sources of shelter and food, but they are also serving as a repository of remedies towards several diseases (Eddouks et al., 2012; Ibrahim et al., 2022). Recently, it has been discovered that many plants' metabolites possess considerable interesting bioactivities; therefore, these metabolites with less toxicity and hazardous influences could have the capacity to replace the synthetic agents and be utilized in food and pharmaceutical industries (Ibrahim et al., 2021; Nobahar et al., 2021; Abdallah et al., 2022). Natural metabolites have gained substantial attentiveness against liver injury because of their diversified bioactivities. A number of studies have demonstrated the hepatoprotection capacity of several phytoconstituents of various classes versus on D-GalN/LPS produced FHF (Xia et al., 2014; Wang et al., 2017; Wang et al., 2018; Wen et al., 2018; Yang et al., 2020). These phytochemicals have shown the ability to modulate oxidative stress, NF-κB pathway, and inflammatory and apoptotic mediators. *Cheilocostus speciosus* (J. Koenig) C.D.Specht (Syn: *C. speciosus*) is a member of the family Costaceae that is widely used in various traditional medicines for treating various ailments: pharyngitis, leprosy, constipation, tonsillitis, pleurisy, rheumatism, flatulence, headache, pneumonia, jaundice, and fever, as well as snake venom antidote (El-Far et al., 2018; Maji et al., 2020). It is also called an insulin plant due to its antidiabetic potential (Maji et al., 2020). Its rhizomes are astringent, bitter, expectorant, aphrodisiac, anthelmintic, and tonic; additionally, they demonstrated antioxidant, antiinflammatory, anthelmintic, hepatoprotective, anticholinesterase, anticancer, antidiabetic, estrogenic, antihyperlipidemic, adaptogenic, antispasmodic, insecticidal, antistress, and diuretic properties (Al-Attas et al., 2015; AlSaadi et al., 2018; Maji et al., 2020; Sirwi et al., 2021; Sirwi et al., 2022). *C. speciosus* is a wealthy pool of various metabolites, including steroids, sesquiterpene lactones, alkaloids, glycosides, phenolics, tannins, flavonoids, and saponins (Al-Attas et al., 2015; Maji et al., 2020). Mokko lactone (ML) is one of the guaianolide sesquiterpenes reported from *C. speciosus* (Al-Attas et al., 2015). Earlier studies demonstrated the potent antioxidative and antiinflammatory capacities of ML against doxorubicin-induced cardio- and hepatotoxicity (Sirwi et al., 2021, 2022). The present study aimed at exploring the potential protection of ML against D-GalN /LPS-induced FHF in mice and investigating its antioxidative and antiinflammatory potentials.

2. Materials and methods

2.1. General procedures

DECA-LCQ spectrometer and AVANCE600-BRUKER were employed for measuring ESIMS and NMR spectra, respectively. Chromatography and TLC analyses were carried out on $SiO_2$60/RP-18 and TLC $SiO_2$60-F_{254} plates, respectively. Visualization of the compound was done utilizing UV (λmax 366 and 255 nm) examination and H_2SO_4/*p*-anisaldehyde reagent spraying.

2.2. Plant material

Plant rhizomes were procured from Saudi local market, Jeddah. The staff members of the Department of Natural Products and Alternative Medicine, Faculty of Pharmacy, King Abdulaziz University Jeddah, Saudi Arabia confirmed the plant's authenticity. A voucher specimen was deposited in the herbarium of the Department under the registration number CS-2-2020 (Sirwi et al., 2022; Sirwi et al., 2021).

2.3. Extraction and isolation of ML

Ten kilograms of dried rhizomes were milled and extracted with $CHCl_3$ (6 × 25 L). The obtained extract was concentrated under vacuum using a rotary evaporator (Heidolph, Schwabach, Germany). The concentrated extract (brown residue, 560 g) was suspended in distilled H_2O (250 mL) and partitioned among *n*-hexane and $CHCl_3$. The concentration of each fraction afforded *n*-hexane (CSHex, 126.0 g) and $CHCl_3$ (CSCH, 345.0 g) fractions. Repeated SiO_2

(0.04–0.063 mm) CC of CSHex fraction (*n*-hexane/EtOAc, 95/5-75/25) gave ML that that was further purified using RP-18 (0.04–0.063 mm) column (H_2O:MeOH gradient) and specified by Co-TLC (precoated TLC plates with SiO_2 60 F254 (0.2 mm) with an authentic sample from our laboratory, besides comparing its spectral data with the published data (Al-Attas et al., 2015).

2.4. Chemicals

LPS and D-GalN (*E. coli* serotype-O111-B4) from Sigma-Aldrich (St. Louis/MO/USA) were dissolved in normal saline. The biochemical kits (e.g., ALP (alkaline-phosphatase), ALT (alanine-amino-transferase), AST (aspartate-amino-transferase), and γ-GT (gamma glutamyl transferase)) were purchased from Human-Gesllschaft fur Diagnostica und Biochemica (Wiesbaden/Germany). Colorimetric kits were purchased for malondialdehyde (MDA, ab233471 Abcam/Cambridge/UK), reduced glutathione (GSH, 354102,100T Calbiochem/MERCK Millipore/Darmstadt/Germany), superoxide dismutase (SOD, ab65354 Abcam/Cambridge/UK), and total antioxidant capacity (TAC, MAK187.1KT, Sigma-Aldrich/St. Louis/MO/USA). Mouse ELISA kits for NF-κB (CSB-E12108m), IL-6 (CSB-E-04639m), TNF-α (CSB-E-04741m), and IL-1β (CSB-E-08054m) were from Cusabio Biotech CO. (Shanghai/China).

2.5. Animals

Adult male Swiss albino mice that weighed 23–27 g were selected and held in standardized circumstances of humidity/temperature/light and dark cycle. The mice had ad libitum access to water and diet. The study protocol and all procedures were approved by the Batterjee Medical College Research Ethical Committee (no. RES-2021-0044), which were in the Laboratory Animal Care Principles (NIH 1985).

2.6. Experimental groups and treatments

To induce FHF, D-GalN (i.p. 700 mg/kg) and LPS (i.p. 10 μg/kg) were injected to mice as previously described (El-Agamy, 2018; Li A et al., 2021). The mice were randomly assigned into 4 experimental groups (n = 8 for each) as follows; Control group where mice were administered only normal saline; LPS/ D-GalN-untreated control where mice were injected with D-GalN and LPS; ML20 + LPS/D-GalN and ML40 + LPS/D-GalN where mice were treated with ML (20 and 40 mg/kg, respectively) for 5 days before LPS/D-GalN challenge.

Eight hours after LPS/D-GalN challenge, the mice were anesthetized using ketamine and then liver and blood samples were gathered. Afterward, the mice were humanely sacrificed. The serum was obtained by centrifuging blood samples at 4000 × *g* at 4 °C for 15 min which was maintained at –80 °C till further analysis. Liver samples were washed with ice-cold saline. Small pieces of the liver (0.5 g) were homogenized using PBS (phosphate-buffered saline) and then centrifuged at 9000 × *g* for 15 min. The supernatant was collected and retained at –80 °C till analysis. An additional liver sample was excised and fixed in a neutral-buffered formalin solution (10%) for histopathologic and immunohistochemical (IHC) investigation.

2.7. Estimation of parameters of hepatic damage

Serum ALT, AST, γ-GT, and ALP were estimated in serum samples as described in the kit's instructions.

2.8. Histopathological analysis of hepatic tissue

Paraffin blocks of liver tissue were sectioned (≈5μm) and stained with H&E (hematoxylin/eosin). Hepatic sections were blindly investigated using a light microscope in random order. As previously described, hepatic inflammatory lesions were graded using five semiquantitative scales (4: severe; 3: moderate; 2: slight; 1: very slight; and 0: no change) (El-Agamy et al., 2018).

2.9. Estimation of oxidative stress marker

MDA assay depends on generating a colored product by reaction with thiobarbituric acid, which can be estimated at 532 nm colorimetrically.

2.10. Estimation of antioxidants

GSH and SOD were estimated utilizing the detection kit's provided protocol. In brief, a piece of the hepatic tissue was washed in NaCl (0.9%) solution, blotted dry, weighed, minced in ice-cold MPA solution, and then centrifuged (10 min/3000 × *g*/4 °C). The supernatants were gathered and retained at 4 °C for the assay. For GSH, a reaction was permitted among 4-chloro-1-methyl-7-trifluromethyl-quinoliniummethylsulfate and all mercaptans (RSH) that existed in the supernatants, followed by β-elimination reaction under alkaline condition (30% NaOH), resulting in a chromophoric thione formation with absorbance maxima at 400 nm. For SOD, the samples were mixed with both enzyme working solution and WST-1 and incubated for 20 min at 37 °C to form a formazan dye which was assessed by absorbance increase at 450 nm. The more SOD activity in the sample, the less formazan dye is produced. For TAC, the samples were mixed with Cu^{2+} working solution and incubated for 90 min at 25 °C, and then the absorbance was measured at 570 nm.

2.11. IHC analysis

The paraffin sections of the liver were dewaxed and processed as previously described (El-Agamy et al., 2018). The sections were IHC-stained using the primary antibodies: rabbit polyclonal antibody against NF-kB p65 (1:200, Fisher Scientific Inc., Waltham, MA, USA) and TNF-α (1:100, Fisher Scientific Inc. Waltham, MA, USA). Diaminobenzidine (DAB) was used for visualization.

2.12. Estimation of NF-κB and cytokines

Hepatic NF-κB, TNF-α, IL-6, and IL-1β levels were determined in the hepatic tissue as claimed by kit manufacturer's protocols.

2.13. Statistical analysis

The presented data are the means ± SE for 8 mice per group. Experimental groups were statistically compared utilizing ANOVA (one-way-analysis of variance) and Tukey's Kramer multiple comparison test. Analysis of histopathological grading was accomplished by the nonparametric Kruskal–Wallis test and Dunn's test. $p < 0.05$ was assigned as significant.

3. Results

3.1. Identification of ML

ML was separated from the dried rhizomes $CHCl_3$ extract using SiO_2 and RP-18 CC (column chromatography) and characterized by various spectral tools (^1H and ^{13}C NMR and ESIMS) as formerly stated (Al-Attas et al., 2015; Sirwi et al., 2021, 2022) (Figure 1).

The obtained NMR data of ML are in agreement with the previously reported data (Sirwi et al., 2021) (Table).

3.2. ML attenuates serum and pathological indices of FHF

As presented in Figure 2, D-GalN/LPS challenge induced a notable rising in serum transaminases (ALT and AST), γ-GT, and ALP levels comparing to the control group indicating damage of the hepatocytes. ML pretreatment remarkably diminished the rise in the abovementioned serum markers of hepatic damage comparing with the LPS/D-GalN group.

The pathological investigation of the hepatic tissue showed the deterioration of the hepatic architecture in the LPS/D-GalN group in comparison to the control group normal histology (Figure 3). The liver of D-GalN/LPS-treated mice exhibited inflammatory changes, focal necrosis, and apoptosis. In contrast, ML-pretreated animals showed significant alleviation of LPS/D-GalN-caused hepatic lesions that was most noticeable in the ML40 + LPS/D-GalN group.

3.3. ML suppressed D-GalN/LPS-caused hepatic oxidative stress and enhanced hepatic antioxidants

LPS/D-GalN injection markedly increased ($p < 0.001$) the hepatic oxidative stress marker MDA contaminant with significant depression of GSH content, SOD activity, and TAC content ($p < 0.001$) comparing to the control group. ML pretreatment efficiently suppressed MDA levels and elevated the levels of GSH, SOD, and TAC compared to the LPS/D-GalN group (Figure 4).

3.4. ML ameliorated NF-κB/downstream cytokine signaling

As presented in Figure 5, D-GalN/LPS administration resulted in activation of NF-κB as it increased its protein immunoexpression and its level in the hepatic tissue compared to the normal mice. Furthermore, D-GalN/LPS increased the levels of TNF-α, IL-6, and IL-1β as well as the immunoexpression of TNF-α compared to the control mice (Figure 6). On the contrary, ML pretreatment significantly hindered the activation of NF-κB as there was a significant amelioration in its immunoexpression and its level in hepatic tissue compared to D-GalN/LPS group. Moreover, the immunoexpression of TNF-α was significantly lowered as well as the levels of the inflammatory cytokines compared to the D-GalN/LPS group.

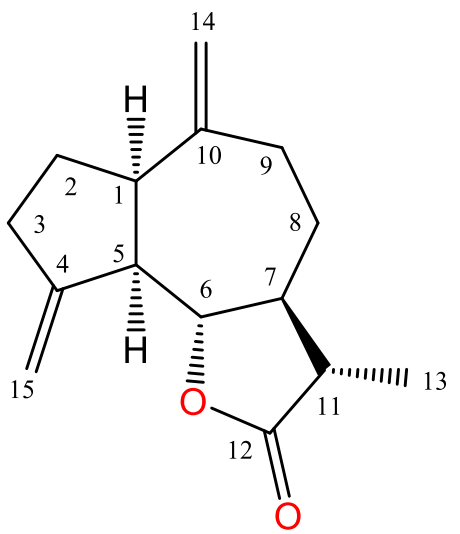

Chemical Formula: $C_{15}H_{20}O_2$

Figure 1. Chemical structure of mokko lactone.

Table . NMR data of ML (600 and 150 MHz, $CDCl_3$).

No.	δ_H (mult., *J* (Hz)	δ_C (mult.)
1	2.88 m	47.1 CH
2	1.92 m 1.83 m	30.2 CH_2
3	2.54 m	32.5 CH_2
4	-	151.2 C
5	2.81 m	52.0 CH
6	3.92 t (10.0)	85.3 CH
7	1.97 m	49.9 CH
8	2.54 m	32.5 CH_2
9	2.48 m 2.11 m	37.7 CH_2
10	-	151.2 C
11	2.21 m	42.1 CH
12	-	178.7 C
13	1.23 d (6.6)	13.2 CH_3
14	4.88 brs 4.78 brs	111.9 CH_2
15	5.20 d (2.4) 5.05 d (2.4)	107.8 CH_2
ESIMS *m/z*: 233 $[M+H]^+$.		

4. Discussion

LPS/D-GalN-induced FHF is a well-established experimental model of severe hepatic damage that is commonly utilized for exploring and investigating the hepatoprotective potential of new therapeutics. The use of the potent inflammagen, LPS, in combination with D-GalN as a promotor of LPS toxic effects, leads to fulminant hepatitis within a few hours that leads to rapid death. LPS is a major constituent of the gram-negative bacteria outer membrane. When injected, it causes inflammatory reaction and overproduction of proinflammatory cytokines, which leads to massive organ damage and failure. D-GalN is an amino sugar, which is metabolized in the liver and depletes hepatic uridine triphosphate and when administered with a subtoxic dose of LPS, mice develop acute hepatic failure (Ma et al., 2015).

C. speciosus is among the commonly used medicinal plants, which was reported to exert hepatoprotective capacity. It was found that its rhizomes' EtOH and MeOH extracts demonstrated marked hepatoprotection on CCl_4- and paracetamol-caused liver injury in rats (AlSaadi et al., 2018; Verma and Khosa, 2009).

ML is a promising phytochemical of *C. speciosus*; however, not much is known about its therapeutic potential.

ML was reported to have cytotoxic potential versus HL-60 cells and induced cell apoptosis through mitochondrial membrane potential collapse with subsequent caspase-3 activation (Yun et al., 2004). Choi et al. purified ML from *Ainsliaea acefifolia* Sch. Bip. roots that revealed in vitro cytotoxic potential versus SK-OV-3, A549, SK-MEL-2, XF498, and HCT15 (ED_{50} ranged from 1.05–2.72 μg/mL) (Choi et al., 2006). ML possessed notable PTP1B (protein-tyrosine phosphatase-1B) inhibition capacity (IC_{50} 1.41 μg/mL) compared to ursolic acid (IC_{50} 0.7 μg/mL) and RK-682 (IC_{50} 1.2 μg/mL), suggesting its potential for treating obesity and diabetes (Choi et al., 2008). Al-Attas et al. stated the antiinflammation capacity of ML as it reduced (IL-6 and -1β, and TNF-α levels with lowering COX-2 and LOX-5 with subsequent decline of PGE2 production (Al-Attas et al., 2015). Sirwi et al. examined ML protective potential versus DOX (doxorubicin)-induced cardio- and hepatotoxic effects. The findings demonstrated its marked protective potential on DOX-caused cardiac injury through its antiinflammation, antioxidant, and anti-apoptotic effectiveness, whereas it prevented DOX-caused liver damage via FOXO1/ Sirt-1/NF-κB axis regulation (Sirwi et al., 2021; Sirwi et al., 2022).

The present results revealed, for the first time, the potential hepatoprotective activity of ML against LPS/D-GalN-induced FHF which may be linked to its potent antiinflammation and antioxidative activities.

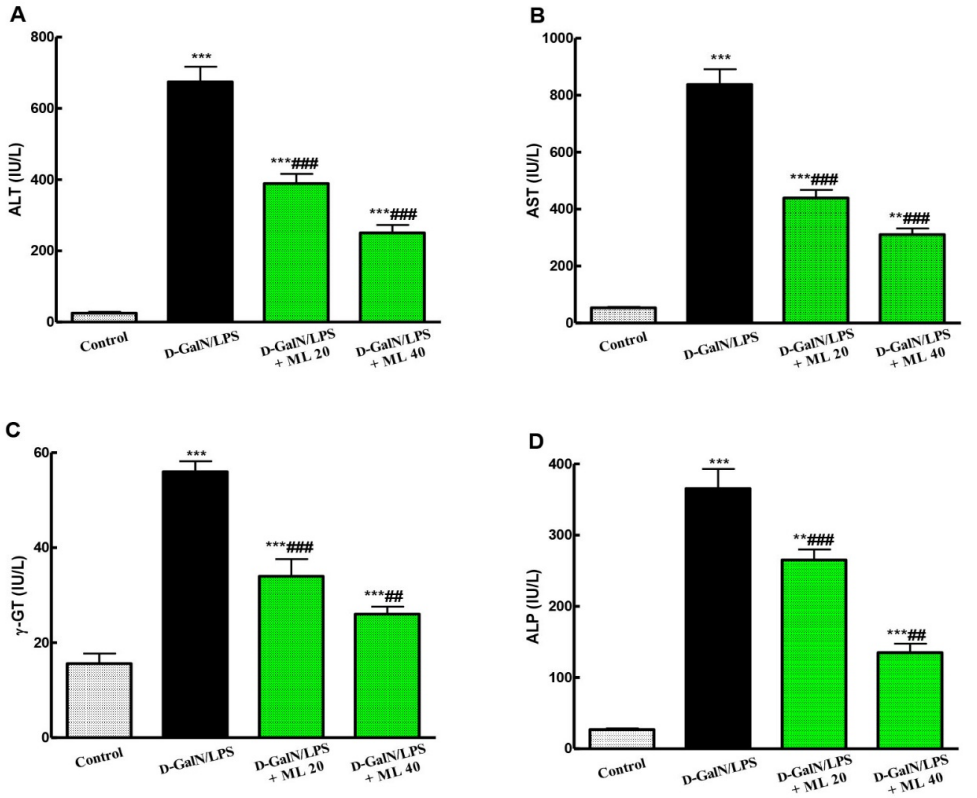

Figure 2. ML attenuated D-GalN/LPS-induced increase in serum indices of fulminant hepatic failure.

A. ALT: Alanine aminotransferase; B. AST: Aspartate aminotransferase; C. γ-GT: gamma glutamyl transferase; D. ALP: Alkaline phosphatase; Data are mean ± SE, n = 8. * P<p < 0.05, ** P<p < 0.01, *** P<p < 0.001 as compared to the control group, #P<p < 0.05, ##P<p < 0.01, ###P<p < 0.001 compared to D-GalN/LPS group (One-way ANOVA).

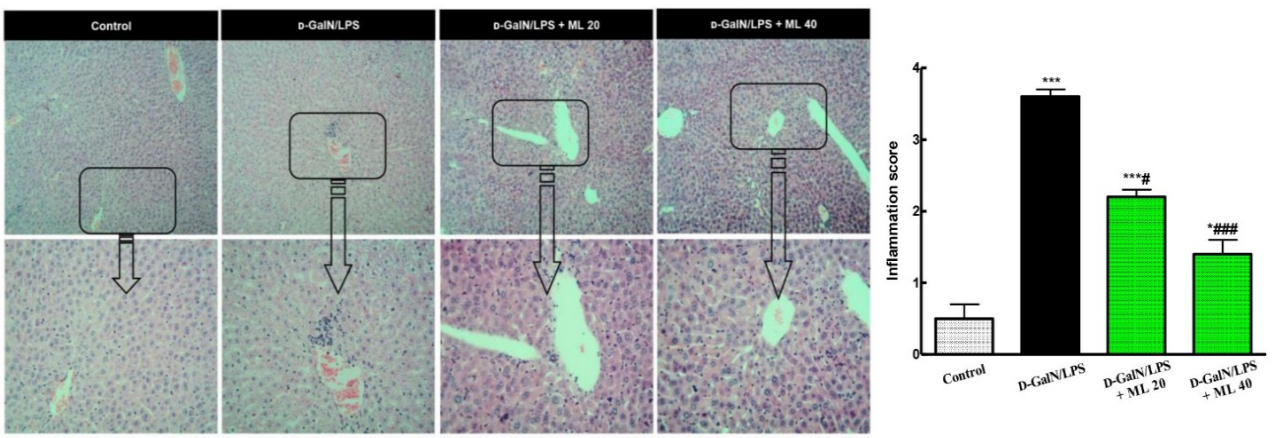

Figure 3. ML attenuated D-GalN/LPS-induced hepatic lesions.

Histopathological captions of hepatic tissue of control mice showing normal architecture, GalN/LPS showing severe inflammation and necrotic areas, ML + GalN/LPS mice showing a significant degree of improvement in hepatic lesions. HE, magnification 100× &200×. F. Inflammatory scores of the hepatic specimen. Data are mean ± SE, n = 8.

$^{*}p < 0.05$, $^{**}p < 0.01$, $^{***}p < 0.001$ as compared to the control group, $^{\#}p < 0.05$, $^{\#\#}p < 0.01$, $^{\#\#\#}p < 0.001$ compared to D-GalN/LPS group (Kruskal–Wallis test).

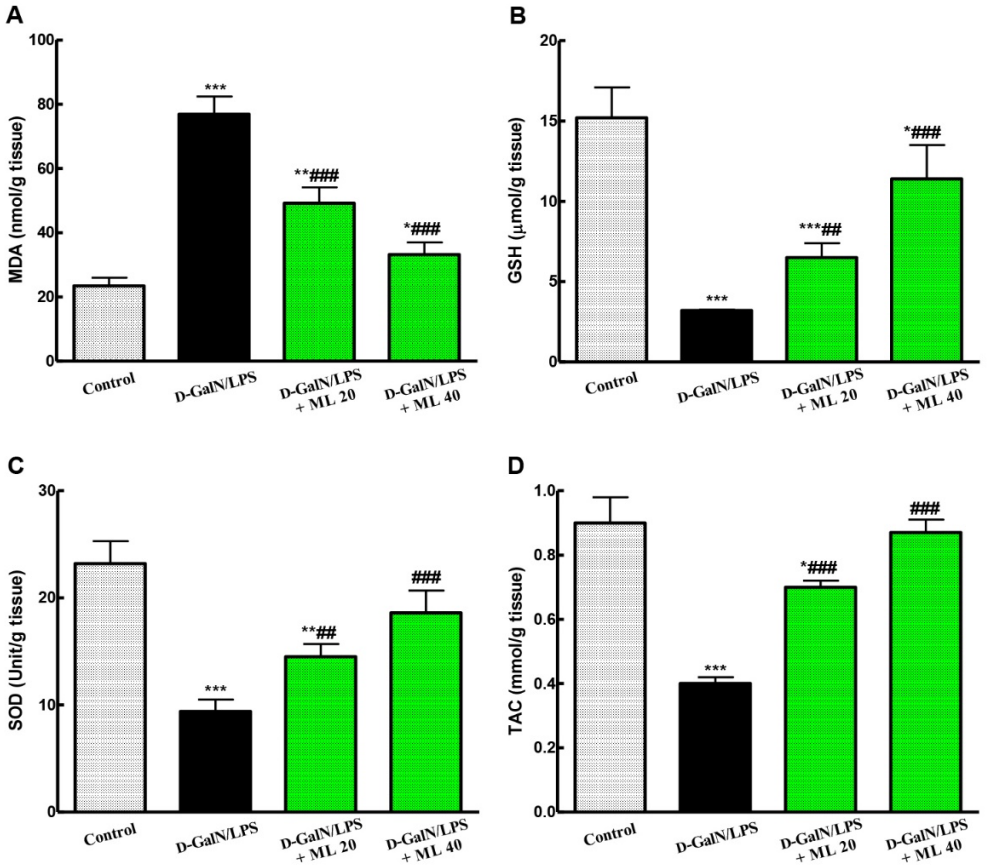

Figure 4. ML suppressed D-GalN/LPS-induced hepatic oxidative stress and enhanced hepatic antioxidants.

A. MDA: Malondialdehyde; **B**. GSH; Reduced glutathione; **C.** SOD: Superoxide dismutase; **D**. TAC: Total antioxidant capacity. Data are expressed as means ± SE, n=8; * $p < 0.05$, *** $p < 0.001$ compared to the control group, $^{\#\#}$ $p < 0.01$, $^{\#\#\#}$ $p < 0.001$ compared to the D-GalN/LPS group (one-way ANOVA).

As presented in the results, D-GalN/LPS injection caused severe hepatocyte death evident by the significant elevation of the cytosolic enzymes i.e. transaminases, γ-GT, and ALP in serum. The biochemical results were supported by the hepatic histopathological examination which showed deleterious focal necrosis, severe portal inflammation, and apoptosis after D-GalN/LPS challenge. These data are in the same line as the previous studies that reported the deleterious hepatic damage following D-GalN/LPS challenge (Liao et al., 2021; El-Agamy et al., 2018; 2014). Pretreatment with ML showed potent hepatoprotective effect that was evident in the significant melioration of hepatotoxicity serum indices concurrent with an improvement of the histopathological hepatic lesions indicating its ability to maintain the integrity of the hepatic tissue as a phytochemical; not much is known about its effects on the molecular pathways of cellular lesions. Hence, its effect on LPS/D-GalN -produced oxidative stress and inflammatory response in the hepatic tissue was investigated.

D-GalN/LPS injection result in a deleterious state of oxidative stress in hepatic tissue due to ROS overproduction which directly depletes GSH, and other antioxidants stores and causes injurious lipid peroxidation (Dong et al., 2017; Fu et al., 2018; Gao et al., 2019; Wen et al., 2018). In line with the previous studies, our data confirmed the increase in lipid peroxidative marker MDA and the suppression of hepatic antioxidants as GSH, SOD, and TAC after LPS/D-GalN injection. Notably, ML pretreatment decreased MDA content and boosted the liver antioxidant capacity through significant elevation of GSH, SOD, and TAC in the hepatic tissue. These results are in line with those of the recent study by Sirwi et al. which stated the ability of ML to alleviate the oxidative burden during doxorubicin-induced hepatotoxicity (Sirwi et al., 2021). Thus, the antioxidative ability of ML may participate in its hepatoprotective potential.

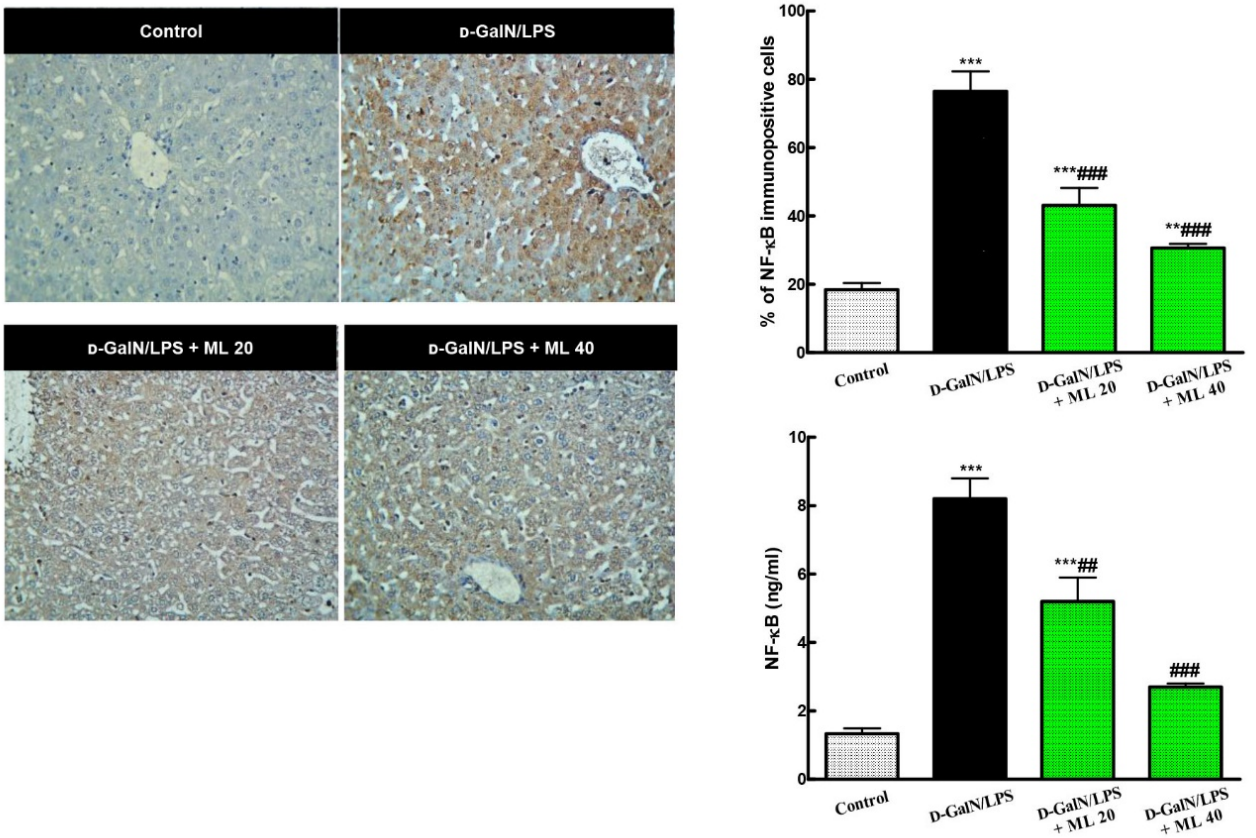

Figure 5. ML ameliorated D-GalN/LPS-induced nuclear factor- κB (NF-κB) activation.

Immunohistochemical staining of NF-κB in the hepatic sections (100×&200×) of the control group showed minimal NF-κB positive staining compared to the increased staining in the D-GalN/LPS group. ML-pretreated groups exhibited significant amelioration in NF-κB staining; Level of NF-κB in the hepatic tissue. Data are expressed as means ± SE, n=8; $^{*}p < 0.05$, $^{**}p < 0.01$, $^{***}p < 0.001$ compared to the control group; $^{\#}p < 0.05$, $^{\#\#}p < 0.01$, $^{\#\#\#}p < 0.001$ compared to the D-GalN/LPS group (one-way ANOVA).

Many previous reports focused on the pivotal role of the transcription factor, NF-κB in the mediation and the provoking of D-GalN/LPS-induced inflammatory response. In the normal state, NF-κB is captured by its inhibitory protein and resided in the cytoplasm. Upon activation, NF-κB is released and enters the nucleus where it stimulates the expression of proinflammatory cytokines as TNF-α and different ILs. D-GalN/LPS challenge is known to be a potent stimulus of NF-κB activation and its translocation into the nucleus which results in the enhanced genetic expression of inflammatory cytokines (Ge et al., 2018; Wang W et al., 2018; Wang X et al., 2019). Furthermore, TNF-α, as a pivotal inflammatory mediator, causes direct hepatocyte damage and promotes hepatocytes apoptosis in the early stage of FHF of D-GalN/LPS-sensitized mice (El-Agamy et al., 2018). TNF-α binds to a specific TNF receptor on the surface of hepatocytes and stimulates inner oxidative stress which results in enhancement of the apoptotic pathway and massive hepatocyte death (Yang et al., 2020). In line with the aforementioned studies, the current results confirmed the increase in NF-κB and its downstream inflammatory cytokines after D-GalN/LPS injection. This inflammatory cascade was interrupted in ML-pretreated mice. These results confirm the data of the previous studies of Sirwi et al. which demonstrated the potent inhibitory effects of ML on NF-κB activation in doxorubicin-induced-hepatotoxicity and cardiotoxicity (Sirwi et al., 2021; Sirwi et al., 2022). Thereupon, it is reasonable to hypothesize that the hepatoprotective property of ML may be partly due to modulation of NF-κB/inflammatory cytokine cascade signaling resulting in alleviation of the inflammatory response. It is noteworthy that other related sesquiterpenes as deoxyelephantopin (Huang et al., 2013), β-caryophyllene (Choi JW et al., 2014) and costunolide (Wang Y et al., 2017) have shown hepatoprotective potential against D-GalN/LPS-induced FHF. These reports attributed this effect due to their abilities to modulate oxidative inflammatory responses. However, further investi-

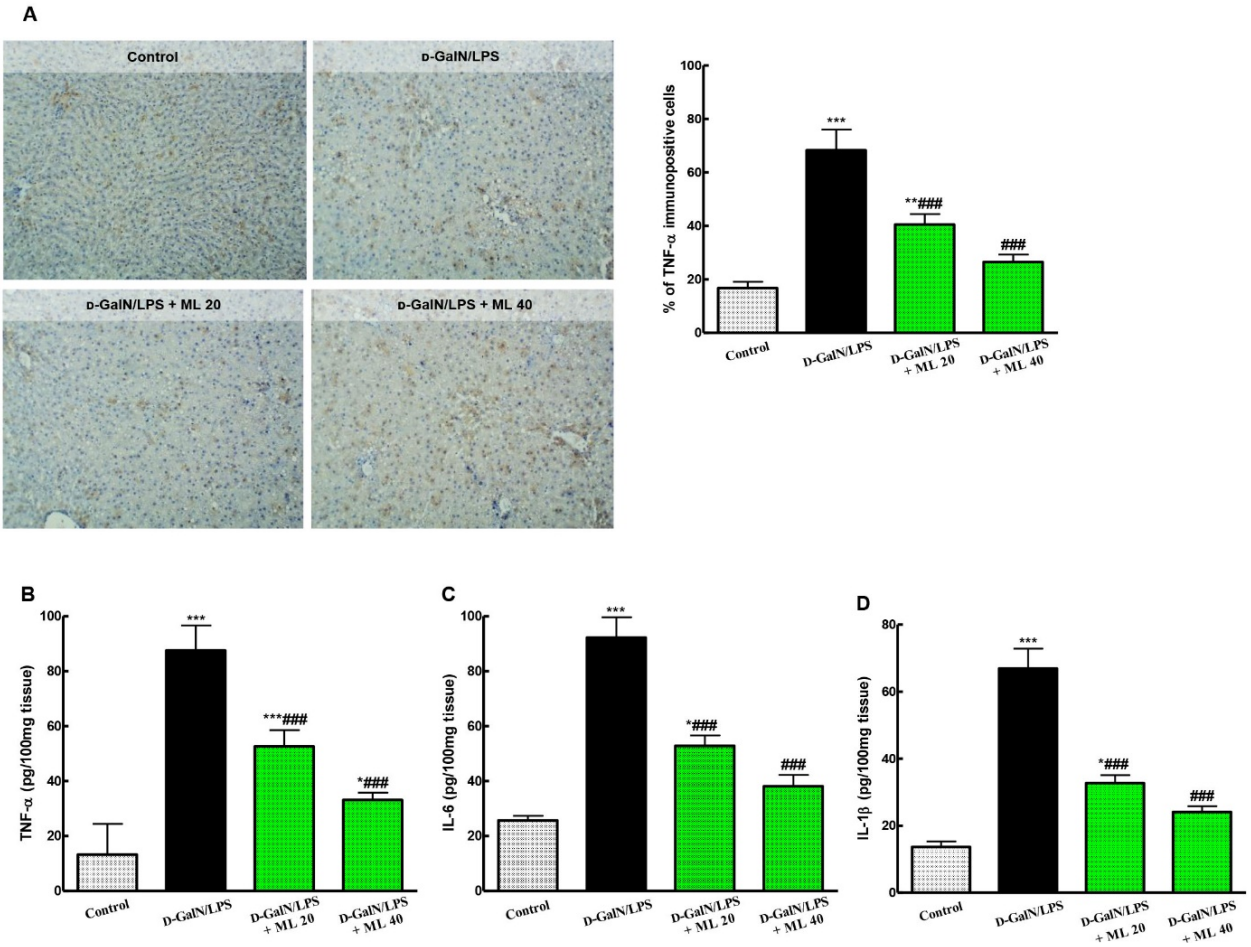

Figure 6. ML lowered D-GalN/LPS-induced cytokine production.

TNF-α: Tumor necrosis factor-α; IL-6: Interleukine-6; IL-1β: Interleukine-1β. A. Immunostaining of TNF-α in the hepatic sections (100×) showing minimal staining in the control group and intensified staining in the D-GalN/LPS group. ML-pretreated groups showed much lower TNF-α positive staining. B. Levels of inflammatory cytokines in the hepatic tissue. Data are expressed as means ± SE, n=8; * $p < 0.05$, ** $p < 0.01$, *** $p < 0.001$ compared to the control group; $^{\#}p < 0.05$, $^{\#\#}p < 0.01$, $^{\#\#\#}p < 0.001$ compared to the D-GalN/LPS group (one-way ANOVA).

gation of ML pharmacological activities is strongly recommended to get a clearer insight to its molecular pathways and confirm its beneficial use for FHF patients.

5. Conclusion

Collectively, the present study demonstrated the hepatoprotective activities of ML against D-GalN/LPS-caused FHF that may be related to its potent antioxidant and antiinflammation activities which may be in-part explained through its capability to repress the activation of NF-κB/inflammatory cytokine signal pathway. Thus, these data encourage further investigation of other possible molecular pathways that underlie the hepatoprotective effects of ML. Also, additional research is strongly recommended to prove the efficacy of ML in FHF patients.

Author contributions

All authors participated equally in all aspects of the study. Prof. Wael M. Elsaed performed the histopathological and immunohistochemical analysis.

Funding

This project was funded by Batterjee Medical College (BMC), Jeddah, Saudi Arabia, project no. (RES-2021-0044). Therefore, the authors gratefully acknowledge BMC for technical and financial support.

Conflicts of interest

The author(s) declared no potential conflicts of interest with respect to the research, authorship, and/or publication of this article.

List of abbreviations

A549	Lung adenocarcinoma cell line
ALP	Alkaline phosphatase
ALT	Alanine-amino-transferase
AST	Aspartate-amino-transferase
BMC	Batterjee Medical College
COX-2	Cyclooxygenase-2
DAB	Diaminobenzidine
DOX	Doxorubicin
FHF	Fulminant hepatic failure
FOXO1	Forkhead box protein O1
γ-GT	Gamma-glutamyltransferase
D-GalN	D-Galactosamine
H&E	Hematoxylin/ eosin
HCT15	Human colorectal carcinoma
HL-60	Human leukemia cell line
IHC	Immunohistochemical
iNOS	Inducible nitric oxide synthase
IFN-γ	Interferon gamma
IL-6	Interleukin 6
IL-1β	Interleukin 1β
5-LOX	5-Lipoxygenase
LPS	Lipopolysaccharide
MDA	Malondialdehyde
ML	Mokko lactone
NF-κB	Nuclear- factor kappa-B
PGE2	Prostaglandin E2
PTP1B	Protein-tyrosine phosphatase-1B
RP-18	Reversed phase -18
SiO2 CC	Silica gel column chromatography
SIRT1	Sirtuin 1
SK-OV-3	Ovarian cancer cell line
SK-MEL-2	Human melanoma cell line
SOD	Superoxide dismutase
TAC	Total antioxidant capacity
TLR-4	Toll-like-receptor-4
TNF-α	Tumor-necrosis factor-alpha
UDP	Uridine diphosphate
XF498	Human CNS solid tumor

References

Abdallah HM, Mohamed GA, Ibrahim SR (2022). *Lansium domesticum*-A fruit with multi-benefits: Traditional uses, phytochemicals, nutritional value, and bioactivities. Nutrients 14: 1531.

Akbar S (2020). Handbook of 200 Medicinal Plants: A Comprehensive Review of their Traditional Medical Uses and Scientific Justifications, Springer Cham, Springer Nature Switzerland AG, pp. 1-14.

Al-Attas AA, El-Shaer NS, Mohamed GA, Ibrahim SR, Esmat A (2015). Anti-inflammatory sesquiterpenes from *Costus* speciosus rhizomes. Journal of Ethnopharmacology 176: 365-74.

AlSaadi BH, AlHarbi SH, Ibrahim SR, El-Kholy AA, El-Agamy DS et al. (2018). Hepatoprotective activity of Costus speciosus (koen. ex. retz.) against paracetamol induced liver injury in mice. African Journal of Traditional, Complementary and Alternative Medicines 15: 35-41.

Choi JW, Park JH, Cho HI, Kwak JH, Lee DU et al (2014). B-caryophyllene protects against D-galactosamine and lipopolysaccharide-induced hepatic failure. Planta Medica 80: P2O28.

Choi JY, Na M, Hyun Hwang I, Ho Lee S, Young Bae E et al. (2008). Isolation of betulinic acid, its methyl ester and guaiane sesquiterpenoids with protein tyrosine phosphatase 1B inhibitory activity from the roots of Saussurea lappa CB clarke. Molecules 14: 266-72.

Choi SZ, Yang MC, Choi SU, Lee KR (2006). Cytotoxic terpenes and lignans from the roots of *Ainsliaea acerifolia*. Archives of Pharmacal Research 29:203-8.

Dong L, Yin L, Quan H, Chu Y, Lu J (2017). Hepatoprotective effects of kaempferol-3-O-α-l-arabinopyranosyl-7-O-α-l-rhamnopyranoside on D-galactosamine and lipopolysaccharide caused hepatic failure in mice. Molecules 22:1755.

Eddouks M, Chattopadhyay D, De Feo V, Cho WC (2012). Medicinal plants in the prevention and treatment of chronic diseases. Evidence-Based Complementary and Alternative Medicine 2012:458274.

El-Agamy DS, Shebl AM, Shaaban AA (2018). Modulation of D-galactosamine /lipopolysacharride-induced fulminant hepatic failure by nilotinib. Human & Experimental Toxicology 37:51-60.

El-Agamy DS, Makled MN, Gamil NM. 2014. Protective effects of agmatine against D-galactosamine and lipopolysaccharide-induced fulminant hepatic failure in mice. Inflammopharmacology 22:187-94.

El-Far A, Shaheen H, Alsenosy A, El-Sayed Y, Al Jaouni S et al. (2018). *Costus* speciosus: Traditional uses, phytochemistry, and therapeutic potentials. Pharmacognosy Review 12:120-7.

Fu T, Li H, Zhao Y, Cai E, Zhu H et al. (2018). Hepatoprotective effect of α-mangostin against lipopolysaccharide/d-galactosamine-induced acute liver failure in mice. Biomedicine & Pharmacotherapy 106:896-901.

Gao K, Liu F, Chen X, Chen M, Deng Q et al. (2019). Crocetin protects against fulminant hepatic failure induced by lipopolysaccharide/dgalactosamine by decreasing apoptosis, inflammation and oxidative stress in a rat model. Experimental and Therapeutic Medicine 18:3775-82.

Ge P, Yao X, Li J, Jiang R et al. (2018). Diminazene aceturate alleviated lipopolysaccharide/D-galactosamine-induced fulminant hepatitis in mice. Biomedicine & Pharmacotherapy 98:142-8.

Gong X, Luo F, Zhang L, Li H, Wu M et al. (2010). Tetrandrine attenuates lipopolysaccharide-induced fulminant hepatic failure in D-galactosamine-sensitized mice. International Journal of Immunopharmacology 10:357-63.

Huang C, Lin K, Cheng Y, Hsu C, Yang S et al. (2013). Hepatoprotective effect and mechanistic insights of deoxyelephantopin, a phyto-sesquiterpene lactone, against fulminant hepatitis. Journal of Nutritional Biochemistry 24:516-30.

Ibrahim SRM, Bagalagel AA, Diri RM, Noor AO, Bakhsh HT et al. (2022). Phytoconstituents and pharmacological activities of Indian camphorweed (*Pluchea indica*): A multi-potential medicinal plant of nutritional and ethnomedicinal importance. Molecules 27:2383.

Ibrahim SR, Altyar AE, Sindi IA, El-Agamy DS, Abdallah HM et al. (2021). Kirenol: A promising bioactive metabolite from Siegesbeckia species: A detailed review. Journal of Ethnopharmacology 281:114552.

Kumar M, Rawat S, Nagar B, Kumar A, Pala NA et al. (2021). Implementation of the use of ethnomedicinal plants for curing diseases in the Indian Himalayas and its role in sustainability of livelihoods and socioeconomic development. International Journal of Environmental Research and Public Health 18 (4):1509.

Li A, Yang Q, Lou G, Liu Y, Xia H et al. (2021). 5-((7-chloro-6-fluoro-1h-indol-3-yl) methyl)-3-methylimidazolidine-2, 4-dione as a RIP1 inhibitor protects LPS/D-galactosamine-induced liver failure. Life Science 273:119304.

Li R, Yang W, Yin Y, Zhang P, Wang Y et al. (2021). Protective role of 4-octyl itaconate in murine LPS/D-GalN-induced acute liver failure via inhibiting inflammation, oxidative stress, and apoptosis. Oxidative Medicine and Cellular Longevity 2021:9932099.

Liao H, Du S, Jiang T, Zheng M, Xiang Z et al. (2021). UMSCs attenuate LPS/D-GalN-induced acute liver failure in mice by down-regulating the MyD88/NF-κB pathway. Journal of Clinical and Translational Hepatology 9:690.

Lyu Z, Ji X, Chen G, An B. (2019). Atractylodin ameliorates lipopolysaccharide and d-galactosamine-induced acute liver failure via the suppression of inflammation and oxidative stress. International Immunopharmacology 72:348-57.

Ma L, Gong X, Kuang G, Jiang R, Chen R et al. (2015). Sesamin ameliorates lipopolysaccharide/d-galactosamine-induced fulminant hepatic failure by suppression of toll-like receptor 4 signaling in mice. Biochemical and Biophysical Research Communications 461:230-6.

Maji P, Dhar DG, Misra P, Dhar P (2020). Costus speciosus (koen ex. retz.) sm.: Current status and future industrial prospects. Industrial Crops and Products 152:112571.

Mohamadi-Zarch S, Baluchnejadmojarad T, Nourabadi D, Ramazi S, Nazari-Serenjeh M et al. (2021). Esculetin alleviates acute liver failure following lipopolysaccharide/D-galactosamine in male C57BL/6 mice. Iranian Journal of Medical Sciences 46:373.

Nobahar A, Carlier JD, Miguel MG, Costa MC (2021). A review of plant metabolites with metal interaction capacity: A green approach for industrial applications. Biometals 34 (4):761-93.

Sirwi A, Shaik RA, Alamoudi AJ, Eid BG, Elfaky MA et al. (2022). Mokko lactone alleviates doxorubicin-induced cardiotoxicity in rats via antioxidant, anti-inflammatory, and antiapoptotic activities. Nutrients 14:733.

Sirwi A, Shaik RA, Alamoudi AJ, Eid BG, Kammoun AK et al. (2021). Mokko lactone attenuates doxorubicin-induced hepatotoxicity in rats: Emphasis on sirt-1/FOXO1/NF-κB axis. Nutrients 13:4142.

Süntar I (2020). Importance of ethnopharmacological studies in drug discovery: Role of medicinal plants. Phytochemistry Reviews 19:1199-209.

Tao Y, Wang M, Wu D, Luo C, Tang H et al. (2019). Apolipoprotein A5 alleviates LPS/D-GalN-induced fulminant liver failure in mice by inhibiting TLR4-mediated NF-κB pathway. Journal of Translational Medicine 17:151.

Verma N, Khosa RL (2009). Evaluation of protective effects of ethanolic extract of *Costus* speciosus (koenig) sm. rhizomes on carbon tetrachloride induced hepatotoxicity in rats. Natural Product Radiance 8:123-6.

Wang W, Wu L, Li Q, Zhang Z, Xu L et al. (2018). Madecassoside prevents acute liver failure in LPS/D-GalN-induced mice by inhibiting p38/NF-κB and activating Nrf2/HO-1 signaling. Biomedicine & Pharmacotherapy 103:1137-45.

Wang X, Wu L, Zhang Q, Li L, Xie Y et al. (2019). Methyl 3, 4-dihydroxybenzoate protects against D-galN/LPS-induced acute liver injury by inhibiting inflammation and apoptosis in mice. Journal of Pharmacy and Pharmacology 71:1082-8.

Wang Y, Zhang X, Zhao L, Shi M, Wei Z et al. (2017). Costunolide protects lipopolysaccharide/D-galactosamine–induced acute liver injury in mice by inhibiting NF-κB signaling pathway. Journal of Surgical Research 220:40-5.

Wen J, Lin H, Zhao M, Tao L, Yang Y et al. (2018). Piceatannol attenuates D-GalN/LPS-induced hepatoxicity in mice: Involvement of ER stress, inflammation and oxidative stress. International Immunopharmacology 64:131-9.

WHO (2022). https://www.who.int/initiatives/who-global-centre-for-traditional-medicine. 2022 Accessed 14 September 2022.

Xia X, Su C, Fu J, Zhang P, Jiang X et al. (2014). Role of α-lipoic acid in LPS/d-GalN induced fulminant hepatic failure in mice: Studies on oxidative stress, inflammation and apoptosis. International Immunopharmacology 22:293-302.

Yang S, Kuang G, Zhang L, Wu S, Zhao Z et al. (2020). Mangiferin attenuates LPS/D-GalN-induced acute liver injury by promoting HO-1 in kupffer cells. Frontiers in Immunology 11:285.

Yun YG, Oh H, Oh GS, Pae HO, Choi BM et al. (2004). In vitro cytotoxicity of mokko lactone in human leukemia HL-60 cells: Induction of apoptotic cell death by mitochondrial membrane potential collapse. Immunopharmacology Immunotoxicology 26:343-53.